arXiv:1604.05611v1 [astro-ph.SR] 19 Apr 2016

Trigonometric Parallaxes and Proper Motions of 134 Southern Late M, L, and T Dwarfs from the Carnegie Astrometric Planet Search Program

Alycia J. Weinberger, Alan P. Boss, Sandra A. Keiser

Department of Terrestrial Magnetism, Carnegie Institution for Science, 5241 Broad Branch Road, NW, Washington, DC 20015-1305

Guillem Anglada-Escudé

School of Physics and Astronomy, Queen Mary University of London, 327 Mile End Road, London, E1 4NS

Ian B. Thompson

Carnegie Observatories, Carnegie Institution for Science, 813 Santa Barbara Street, Pasadena, CA 91101-1292

Gregory Burley

National Research Council of Canada, 5071 West Saanich Road, Victoria, BC V9E 2E7, Canada

ABSTRACT

We report trigonometric parallaxes for 134 low mass stars and brown dwarfs, of which 38 have no previously published measurement and 79 more have improved uncertainties. Our survey targeted nearby targets, so 119 are closer than 30 pc. Of the 38 stars with new parallaxes, 14 are within 20 pc and seven are likely brown dwarfs (spectral types later than L0). These parallaxes are useful for studies of kinematics, multiplicity, and spectrophotometric calibration. Two objects with new parallaxes are confirmed as young stars with membership in nearby young moving groups: LP 870-65 in AB Doradus and G 161-71 in Argus. We also report the first parallax for the planet-hosting star GJ 3470; this allows us to refine the density of its Neptune-mass planet. One T-dwarf, 2MASS J12590470-4336243, previously thought to lie within 4 pc, is found to be at 7.8 pc, and the M-type star 2MASS J01392170-3936088 joins the ranks of nearby stars as it is found to be within 10 pc. Five stars that are over-luminous and/or too red for their spectral types are identified and deserve further study as possible young stars.

Subject headings: astrometry – stars: low-mass, brown dwarfs

1. Introduction

Determination of the physical properties of low mass stars and brown dwarfs, most importantly luminosities, depends upon having accurate distances. However, these late-type objects were generally too faint for inclusion in the all-sky Hipparcos survey. Through the efforts of several ground-based astrometric surveys, there are now hundreds of low-mass stars with parallaxes (e.g. Dahn et al. 2002; Jao et al. 2005; Costa et al. 2006; Andrei et al. 2011; Dupuy & Liu 2012; Faherty et al. 2012; Dieterich et al. 2014; Sahlmann et al. 2014; Zapatero Osorio et al. 2014). Nevertheless, there are still many objects within 30 pc without well-measured distances. These nearby, bright objects would be the best templates for studies of radii, atmospheric composition, metalicity, and other spectroscopic properties. In addition, low mass stars with excellent distances provide the templates for spectrophotometric distances to more distant stars.

In 2007, we began a long-term astrometric search for gas giant planets and brown dwarfs orbiting nearby low mass dwarf stars (Boss et al. 2009). The search employs a specialized astrometric camera, the Carnegie Astrometric Planet Search Camera (CAPSCam), with a design optimized for high accuracy astrometry of M dwarf stars. Here we report our trigonometric parallaxes for 134 low mass stars. Of these, 38 have no previously reported measured parallax.

2. Observations

CAPSCam operates on the 2.5-m du Pont telescope at the Las Campanas Observatory in Chile and is described in detail by Boss et al. (2009); its main features for astrometry of low mass stars are briefly described here. CAPSCam has no internal moving parts and employs an astrometric quality filter as its window that is approximately z-band (865 nm with a bandpass of 100 nm). The field of view is 6.7 arcmin on a side, with 2048×2048 pixels each subtending $0\farcs196$. A subarray, also known as the "guide window," is arbitrarily sizable and locatable and may be read out independently from the rest of the field. A bright target star is placed in the guide window, which is then read out fast enough so the star does not saturate while the rest of the pixels integrate on the reference stars; a mechanical shutter in front of the entrance window ensures that the exposure time on the bright star remains, as much as possible, commensurate with that on the full field. Thus, the camera can achieve high dynamic range without excessive overhead.

Target selection concentrated on southern M, L and T dwarfs closer than 20 pc as known from either parallaxes or spectrophotometric distances. At the time of the initial target selection ten years ago, distances and spectral sub-types for many late type stars were lacking, so high proper motion stars were included as well. The earliest spectral type included was M3, and the majority of targets are spectral type M5.5 and later. In 2011,

the target list was updated to include all objects with spectral type later than M4, closer than 12 pc, and south of declination +16°. Stars must have I magnitudes greater than ∼9 so as not to saturate the detector in the minimum guide window exposure time of 0.2 s. The faintest objects we target have I∼18 so as to provide S/N∼500 in a 120 s integration.

Our typical observing strategy is to place target stars brighter than I∼15 in the guide window. Full field integration times are chosen to get at least 6, and typically more like 25, well-exposed reference stars; the number of reference stars for each field is given in Table 1. The typical astrometric reference star for our fields has I∼17 and can be as faint as I∼22. The usual integration times are also given in Table 1, although in some epochs, they were adjusted for seeing and clouds. At each epoch, we typically observe for an hour and thus obtain 20-40 images of the full field. Targets are almost always observed within an hour of transit, and given the long wavelength filter of the camera there is little differential atmospheric refraction as a function of stellar spectral type.

The data for our parallaxes were collected from 2007-2014. The number of epochs per source varies from 4, the minimum to obtain a parallax with uncertainty estimates, to more than 20 for a few well-studied targets. The number of epochs, and the start and end dates for the data, and time baseline of the observations included in the parallaxes are given in Table 1. We typically observe each star at least twice per calendar year. The stars range in spectral type from M3 through T7, with the bulk of the targets being late M-type.

3. Data Reduction

Details of CAPSCam astrometric data reduction may be found in Boss et al. (2009) and Anglada-Escudé et al. (2012) and are briefly summarized here following the description in Weinberger et al. (2013). For each epoch, the x and y pixel positions of the brightest ∼100 stars (more in crowded fields) in the field are found with a centroiding algorithm. Data from all epochs are combined in an astrometric solution to derive the positions, proper motions, and parallaxes of all the cross-matched stars in each target field. The astrometric solution is an iterative process. An initial catalog of positions starts with the centroids from a chosen epoch transformed to sky coordinates based on the coordinates of the target star and the known pixel scale. Next, a transformation is applied to every other epoch's catalog to match the initial catalog, and the apparent trajectory of each star is fit to a basic astrometric model. The parallaxes for all objects are initialized to zero. The initial catalog is updated with new positions, proper motions, and parallaxes, and a subset of well-behaved stars is selected to be used as the reference frame. The reference stars must be successfully extracted in every epoch and a subset of at least 15, and more typically 30, is chosen that shows the smallest epoch-to-epoch variation in their solutions. This process is then iterated a small number of times.

In each iteration the individual parallax and proper motions of every star are adjusted, so the mean parallax should stay at approximately zero. However, the subset of reference stars do not necessarily have mean parallax of zero. At any epoch, the position of a star has centroiding uncertainties, and for distant stars, proper motion will take out all apparent motion of the star, leaving positional residuals that are both positive and negative. Therefore, although the true parallax to every star must be positive, we allow the fit parallaxes to take on positive and negative values.

To assess the uncertainties on the measured parallax, we perform a Monte Carlo where we fit the starting position, parallax, and proper motion in each trial. Each trial draws random positions for each epoch based on the nominal position determined from the iterative solution and its positional uncertainty. If the χ^2 of the parallax fit is >1, we add to every epoch's uncertainties and re-fit until χ^2 equals one. This additional uncertainty, or positional jitter, may arise from any sources of systematic uncertainty. The final parallax uncertainty is the standard deviation in the parallaxes of each trial.

The final astrometric solution gives the motion of all the stars in the field. However, these stars have parallactic motions that are all in the same direction, since they are generated by Earth's motion. This introduces a small bias, also known as a zero-point parallax offset, that must be removed to find the absolute parallax.

To find the zero point for each field, we estimate a photometric distance to the brightest reference stars by fitting a Kurucz stellar model to cataloged USNO-B1 magnitudes at B2, R2, and I (Monet et al. 2003) and 2MASS magnitudes at J, H, and Ks (Skrutskie et al. 2006) and assuming each star is a dwarf. Dwarf stars with fit Teff < 4000 K are excluded. We average the difference between our astrometrically determined (even if they are not statistically significant) and photometric parallaxes to find the average bias and its uncertainty and subtract it from our relative parallaxes and propagate the uncertainty. We cannot make a comparable zero-point proper motion correction because so few stars as faint as our reference stars have measured absolute proper motions. For 18 of our fields, we were unable to compute a zero point correction due to a combination of reference stars that were too cool and/or faint to be fit well. However, inspection of Table 2 shows that our typical zero point correction is small (< 1 mas) and that the average correction across the stars for which they were computed is -0.09 ± 0.43 mas. Therefore, for these 18 objects, we assumed no zero point correction and an additional uncertainty of 0.4 mas.

4. Results

Table 2 lists the relative parallaxes, relative proper motions, zero-point parallax corrections, and final absolute parallaxes for all our targets as well as previously published trigonometric parallax values from the literature. Figure 1 compares our absolute parallaxes

with published parallaxes from other work.

For 79 of the 96 stars with previously published parallaxes, our measurements have lower uncertainty. In general there is very good agreement between ours and previous measurements; only 12 of the 96 disagree by more than 3 σ (of the less accurate measurement), and for 8 of these 12, the difference in parallax is <5%. The remaining four discrepant sources are explained in more detail, below.

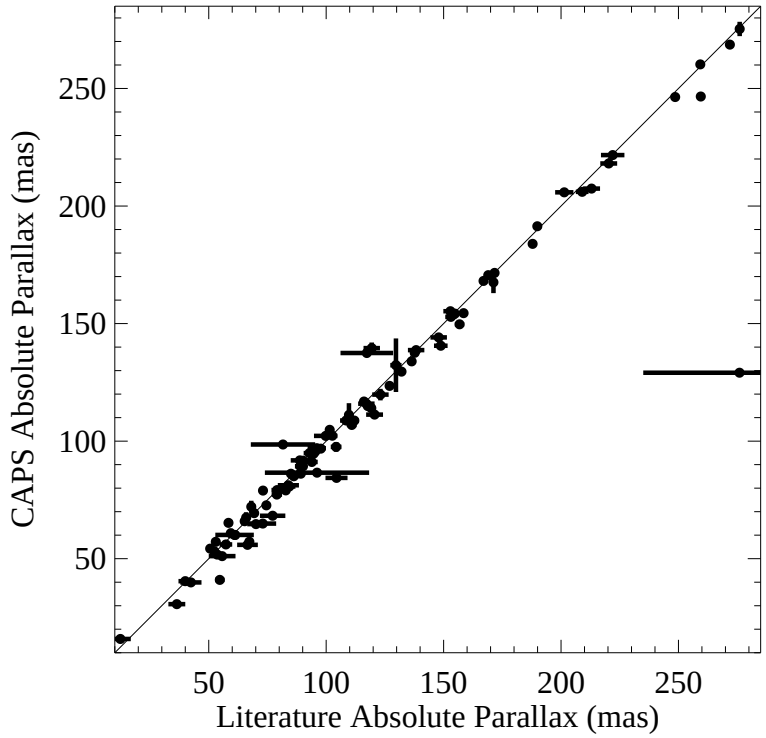

Fig. 1.— A comparison of parallaxes for 95 of the CAPS targets for which literature values exist. The diagonal line is drawn as a guide and is not a fit. The obviously discrepant point is 2MASS J1259-4336, and is discussed in Section 4.1. Not shown is GJ 406, the closest star in our sample, whose parallax is 413 mas.

A formal least-squares fit to the published trigonometric parallaxes versus ours gives a slope of 0.988 ± 0.003, i.e., the CAPSCam parallaxes are slightly low compared to published values – an average of 2.9 mas low. However, the χ^2 of this fit is poor, which suggests that either the literature uncertainties, our uncertainties, or both, are underestimated. Note also that this comparison includes the poor matches addressed below.

There are also 38 targets in Table 2 with no previous trigonometric parallax including 7 stars with spectral types later than M8. A color-magnitude diagram for all the stars in our sample is shown in Figure 2. As expected, most of the new nearby objects have the expected brightnesses and colors of old, field objects. Exceptions are discussed below.

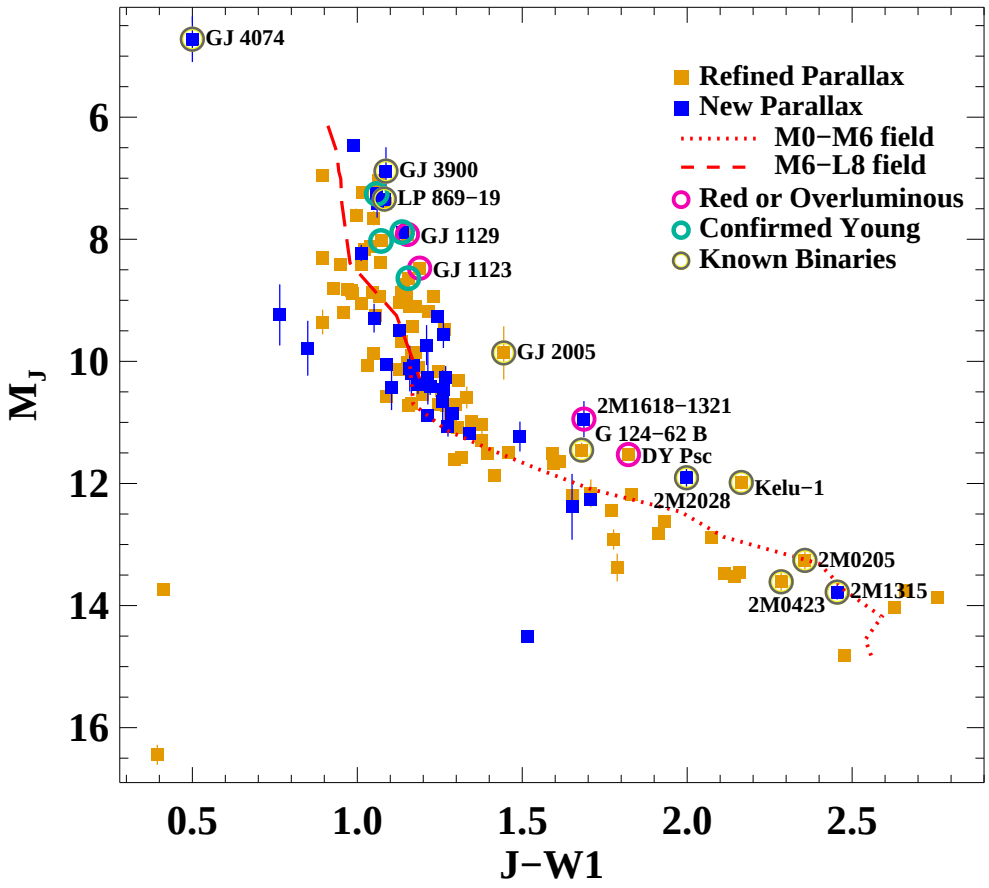

Fig. 2.— The J-W1 (WISE Band 1) versus M_J color-magnitude diagram including all the stars for which we obtained parallaxes. Objects without previously published parallaxes are shown in blue. The M0–M6 field star sequence from Pecaut & Mamajek (2013) is shown in a red dashed line while the M6–L8 field sequence from Faherty et al. (2016) is shown in a red dotted line. Young objects (aqua circles) lie above the sequence; their names are not on the plot to avoid crowding, but they are described in Section 4.2.1. Known binaries (gray/yellow cirlces) generally lie above the field sequence and are listed in Section 4.2.2. Five other sources that are too red for their spectral types and/or overluminous are shown with pink circles and are also discussed in Section 4.2.2.

4.1. Discrepant Sources

GJ 3198: The literature value from Riedel et al. (2010) is 67.3 ± 1.2 and our value is 57.2 ± 1.4. However, our (relative) proper motions agree well: theirs is (483, -486) mas yr^{-1} and ours is (480, -474) mas yr^{-1} . They have a baseline of 5.3 yr and we have a baseline of 4.1 yr. Our parallax fits are shown in Figure 3. So, the source of the parallax discrepancy is unclear, but our parallax factor coverage is very good, particularly in right ascension. With either parallax, the star's position on the color-magnitude diagram is slightly too red for its

absolute magnitude and suggests probably binarity, but the star does not quite make the cuts we impose to find such objects in Section 4.2.2.

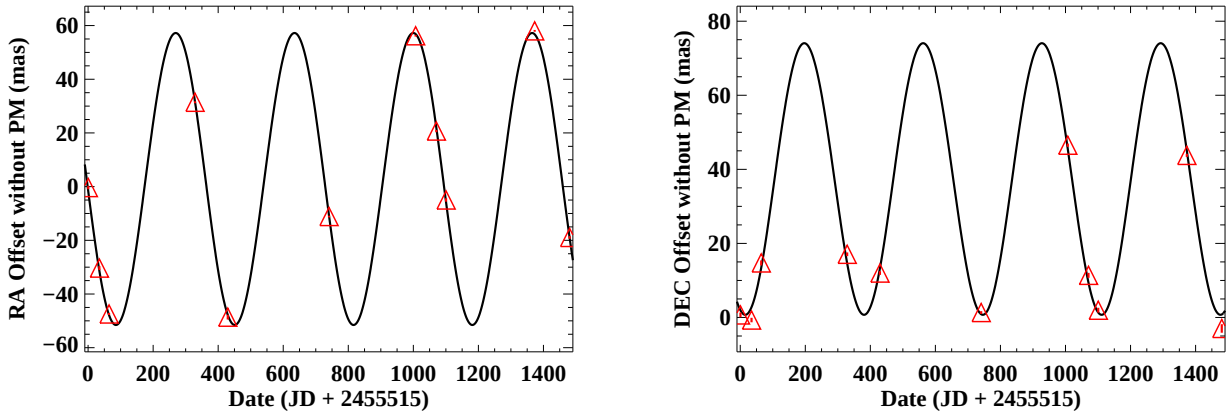

Fig. 3.— Measurements of the motion of GJ 3198 in right ascension and declination after removing the proper motion, which otherwise dominates the scale of the plot. In all the plots shown, the position of the star in the first epoch of observation is taken to be (0,0). Typical per epoch uncertainties are <1 mas and are plotted but not usually visible within the symbols. The best fit parallax is shown with the solid line.

2MASS J115539523727350: Our parallax of 84.4 ± 0.8 is 20% smaller than that of Faherty et al. (2012)'s 104.4 ± 4.7. Again, our relative proper motions agree well: ours is (53.7, -784.49) and theirs is (66.8, -777.9). They had a baseline of 2.5 yr and we have baseline of 7.1 yr. Our parallax fits are shown in Figure 4.

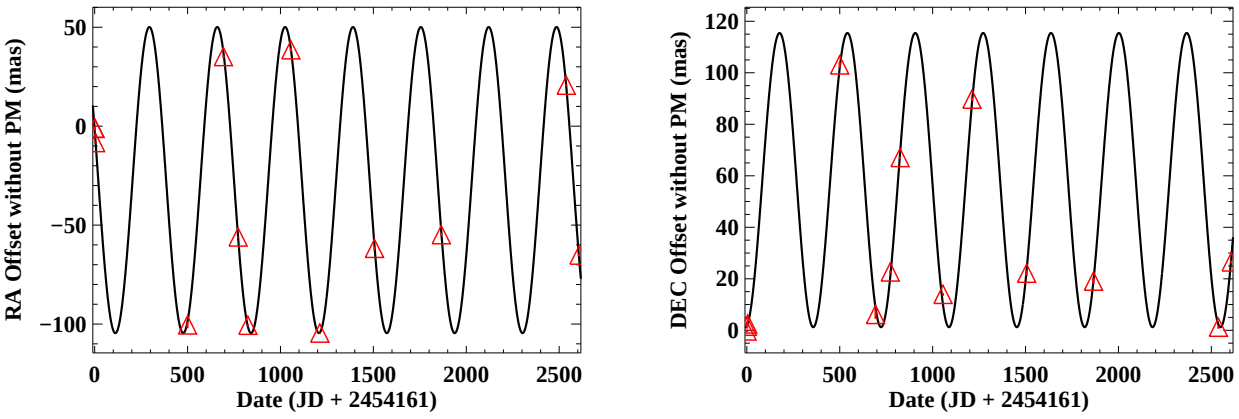

Fig. 4.— Measurements of the motion of 2MASS J11553952-3727350 in right ascension and declination after removing the proper motion, which otherwise dominates the scale of the plot. The best fit parallax is shown with the solid line.

Ruiz (ESO) 207-61: In the table, we gave the average of three literature parallaxes, i.e. 54.7 mas (Ianna & Fredrick 1995; Tinney 1996; van Altena et al. 1995), but the measured values range from 50.4 to 66.1 mas. We get 41.0 ± 1.6 mas. We have dropped this source from our program, so we only have 6 epochs, but they are spread over 5.2 yr with good coverage of the parallax factor. Our parallax fits are shown in Figure 5.

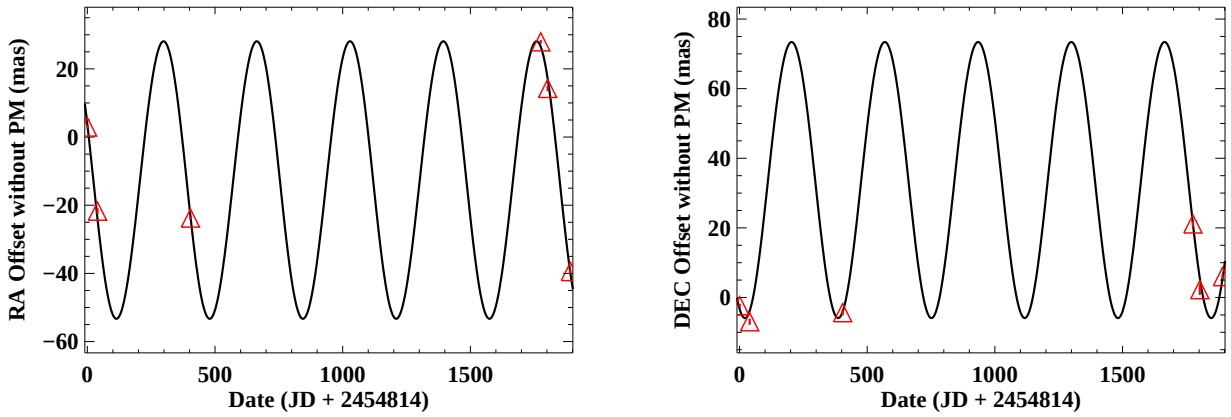

Fig. 5.— Measurements of the motion of ESO 207-61 in ascension and declination after removing the proper motion, which otherwise dominates the scale of the plot. The best fit parallax is shown with the solid line.

2MASS J12590470−4336243: Deacon et al. (2005) found a parallax of 276 ± 41 mas for this object, which they refer to as SIPS1259-4336, based on scanned UKST and ESO plates. They noted that their derived distance (3.6 pc) made the object have an absolute magnitude too bright for a single dwarf, and suggested it could be a binary. However, we find a parallax of 129 mas, which puts the object twice as far away, at 7.8 pc, so it need not be a binary, and its absolute magnitude M_J=11.09 ±0.05 is consistent with its color of J-W1=1.30 ± 0.03 for a single M8. Our proper motion (not adjusted from the apparent value) of 1101.5 ± 1.1 mas yr^{-1} in RA and −253.28 ± 0.30 mas yr^{-1} in DEC agrees quite well with that of Deacon et al.: 1105 ± 4 mas yr^{-1} and −262 ± 4 mas yr^{-1} in RA and DEC respectively. The parallax solution is shown in Figure 6.

4.2. Notes on Interesting Individual Sources

2MASS J01365662+0933473: This nearby brown dwarf, type T2.5, is a benchmark for the study of atmospheric variability and clouds in cool objects (Artigau et al. 2009). It had no previously published parallax. Artigau et al. (2006) found a photometric distance of 6.4 ± 0.3 pc, and our parallax gives a distance consistent with this, namely 6.14 ± 0.04 pc.

2MASS J01392170−3936088: The photometric distance to this source computed

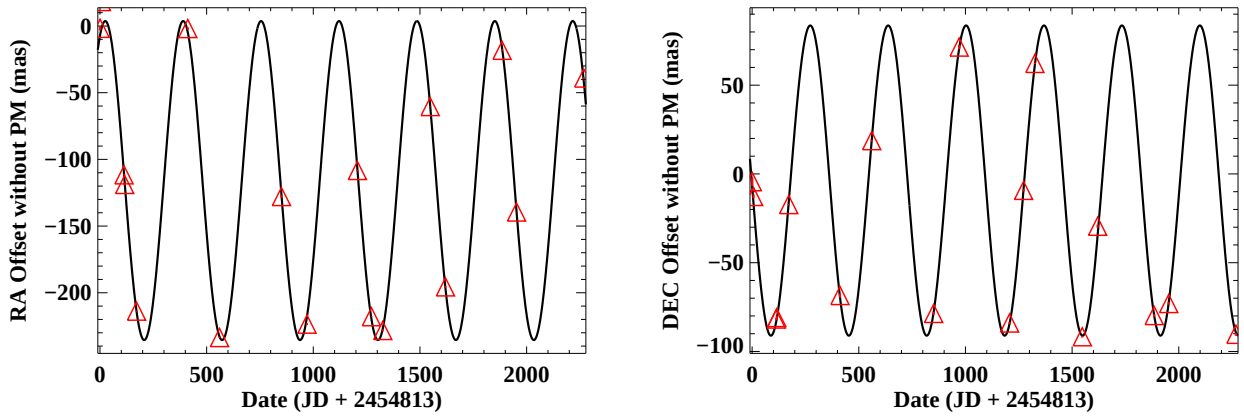

Fig. 6.— Measurements of the motion of 2MASS J12590470-4336243 in right ascension and declination after removing the proper motion, which otherwise dominates the scale of the plot. The best fit parallax is shown with the solid line.

in Deacon & Hambly (2007) is $14.99^{+8.96}_{-5.61}$ pc. Our trigonometric parallactic distance is 8.80±0.04 pc, and the location of the star in the $M_J - (J - W1)$ color-magnitude diagram (Figure 2) does not look unusual. This is now added to the list of stars within 10 pc.

LP 944-20: This is a low-gravity, i.e. likely young, brown dwarf that is not co-moving with a known young association (Faherty et al. 2016). Our parallax of 154.4 ± 0.60 mas confirms the parallax measurement 155.9 ± 1.0 mas of Dieterich et al. (2014) that is markedly different from that of Tinney (1996) (201.4 ± 4.2 mas).

GJ 3470: This nearby M dwarf has a Neptune mass planet detected by radial velocity and transit observations (Bonfils et al. 2012). It has no previously published trigonometric parallax; we get 34.15 ± 0.66 mas or $29.28^{+0.58}_{-0.56}$ pc.

The inferred planetary mass and radius depend sensitively on the stellar properties. Demory et al. (2013) measured a stellar density $\rho_\star = 2.91^{+0.37}_{-0.33}\rho_\odot$ and inferred $M_\star$=$0.539^{+0.047}_{-0.043}$ $M_\odot$, $R_\star$=$0.568^{+0.037}_{-0.031}$ $R_\odot$, and distance=$30.7^{+2.1}_{-1.7}$ pc.

Our new distance is within their uncertainties, but we recompute the best stellar mass and radius with a Monte Carlo that uses our distance and the published photometry. Because of the density measurement, there are two nearly independent methods to find $R_\star$. First, the physical size can be determined from combining our distance with the K-band magnitude, via the angular size relation of Kervella et al. (2004). Second, the stellar mass can be determined from the V, J, H and K-band relations of Delfosse et al. (2000) and combined with the measured $\rho_\star$ of Demory et al. (2013) to determine $R_\star$. We use a Monte Carlo to find the probability densities for both independent estimates and then multiply the probability densities to get the combined best estimate and its uncertainty: $R_\star$=0.550 ± 0.012 $R_\odot$.

Our best stellar radius is again within the uncertainties of the estimate of Demory et al. (2013), but 3.2% smaller on the mean and with smaller uncertainty. This also reduces the inferred radius of the planet by the same amount, and increases the planetary density by 10% to 0.79 g cm^{-3}.

2MASS J20282035+0052265: This is an L-dwarf binary system that was not resolved in HST/NICMOS observations analyzed in Reid et al. (2008) but was resolved using new analysis techniques of the same data in Pope et al. (2013). The latter work found it to be a nearly equal spectral type binary (L3+L4) and estimated a new spectrophotometric distance of 26.1 ± 3.9 pc. Our parallax places the binary at 30.1 ± 1.2 pc. We only have four epochs of data so we cannot say if we observe orbital motion in the astrometric signal; it was dropped from the planet search program for being too far away.

4.2.1. Young Sources

Stars can appear overluminous in the color-magnitude diagram (e.g. Fig. 2) because of youth. The companion to Fomalhaut, LP 876-10 (Mamajek et al. 2013), and AP Col (Riedel et al. 2011) are two examples in Figure 2. We also find two others.

G 161-71: The spectrophotometric distance to this source is typically given as ∼6.7 pc (Reid & Cruz 2002; Scholz et al. 2005; Riaz et al. 2006), but our parallactic distance is 13.26 ± 0.14 pc. Malo et al. (2014) measured an RV of 13.5 ± 0.4 km s^{-1} and listed it as a possible Argus association member. Using our parallax and proper motions combined with this RV, we confirm a 99.99% probability of membership in the 30-50 Myr old Argus association using the BANYAN I tool (Malo et al. 2013). An overluminosity of 1.5 mag is possible for such a young star (Gagné et al. 2015). In addition, the enhanced X-ray luminosity of this star (Riaz et al. 2006) is also consistent with that of other young stars (Shkolnik et al. 2009).

LP 870-65: This is an M4 or M4.5 star with a spectrophotometric distance in Scholz et al. (2005) of 8.7 pc, and our parallactic distance is 18.22 ± 0.19 pc. Indeed, Bowler et al. (2015) identified this star, also known as NLTT 48651, as young based on its X-ray and UV luminosity. That paper also gives a radial velocity of -7.5 ± 0.7 (E. Shkolnik, personal communication) and suggests a tentative association with the AB Dor moving group. Using our parallax and proper motions combined with this RV, the BANYAN I tool confirms a 100% probability of membership in the ∼100 Myr old AB Dor Association.

4.2.2. Overluminous and/or Red Sources

Binaries: Several known binaries are in our sample; those that are equal brightness appear overluminous in Figure 2: GJ 2005 (Leinert et al. 1994), Kelu-1 (Gelino et al. 2006),

G 124-62B Bouy et al. (2003), GJ 3900 (Bonfils et al. 2013), GJ 4074 (Bonfils et al. 2013), LP 869-19 (Malo et al. 2014), 2MASS J20282035+0052265 (Pope et al. 2013), and ϵ Indi B (McCaughrean et al. 2004). The companions to 2MASS J04234858-0414035 (Burgasser et al. 2005) and 2MASS J13153094-2649513 (Burgasser et al. 2011) are T dwarfs and do not cause noticable overluminosity. Suprisingly, 2MASS J02052940-1159296 (Koerner et al. 1999), which is an equal flux ratio binary, does not look overluminous.

In addition to these known binaries, we search for stars that appear overluminous or redder than expected based on their spectral types. For M0 - M6 spectral types, we search for stars that lie redder than the field sequence as given in Pecaut & Mamajek (2013)[1] by more than the combined 1σ uncertainties in the dwarf sequence and the stars' individual color uncertainties. Since Pecaut & Mamajek do not provide uncertainties on the colors, we computed J−W1 for ∼20 stars in each spectral type bin taken from DwarfArchives.org[2]. For M4, M5 and M6 stars, we find a color and dispersion of 1.00 ± 0.06, 1.12 ± 0.08, and 1.16 ± 0.08 mag respetively. We assume a 0.08 mag uncertainty for M0-M3 also. For M7 and later spectral types, we search for stars that lie above the field sequence given in Faherty et al. (2016). Combined, we find four stars that appear overluminous or redder than expected: DY Psc, GJ 1123, GJ 1129, and 2MASS J16184503-1321297.

These stars are peculiar. In principle, they could be candidate young stars. All of these stars have absolute magnitudes that are more than 0.75 mag from their expected values based on their J−W1, so are not just obviously equal brightness binaries. DY Psc is particularly red (J−W1 = 1.82 ± 0.04) for its optically determined spectral type of M9.5 (J−W1 = 1.5). However, none of these stars has X-ray emission detected in the ROSAT all-sky survey (Boller et al. 2016) or were strong UV emitters, at the level of the known young stars, in the GALEX survey.

5. Discussion and Summary

Parallaxes combined with infrared colors can identify interesting low mass stars and brown dwarfs that are young and/or in multiple systems. Only four of the targets in our sample are in the Tycho-2 catalog and would therefore be expected to have full astrometric solutions including parallax in the first GAIA data release in 2016. These are GJ 3379 (M4), G 108-21 (M3.5), GL 452.1 (M4.5), and LTT 7434 (M4).

Thirty-two of the stars here are not part of our long-term monitoring program for any of a number of reasons including: being too far away (π <50 mas), being a close visual binary or stellar spectroscopic binary, or having a bad astrometric reference frame. We are

[1]Updated at `http://www.pas.rochester.edu/$\sim$emamajek/EEM_dwarf_UBVIJHK_colors_Teff.txt`

[2]List of M dwarfs at http://spider.ipac.caltech.edu/staff/davy/ARCHIVE/index.shtml

continuing to observe all the stars that have more than 10 epochs in Table 2.

We thank the staff of Las Campanas Observatory for their ongoing support of this long-term program. Jackie Faherty and Jonathan Gagne provided helpful input. This work has been supported in part by NSF grant AST-0352912, NASA Origins of Solar Systems grant NNX09AF62G, and NASA Astrobiology Institute grant NNA09DA81A. This research has made use of the SIMBAD and Vizier databases, operated at CDS, Strasbourg, France. This publication makes use of data products from the Two Micron All Sky Survey, which is a joint project of the University of Massachusetts and the Infrared Processing and Analysis Center/California Institute of Technology, funded by the National Aeronautics and Space Administration and the National Science Foundation. This publication makes use of data products from the Wide-field Infrared Survey Explorer, which is a joint project of the University of California, Los Angeles, and the Jet Propulsion Laboratory/California Institute of Technology, funded by the National Aeronautics and Space Administration. This publication made use of the Mikulski Archive for Space Telescopes (MAST). STScI is operated by the Association of Universities for Research in Astronomy, Inc., under NASA contract NAS5-26555. Support for MAST for non-HST data is provided by the NASA Office of Space Science via grant NNX09AF08G and by other grants and contracts.

REFERENCES

Andrei, A. H., Smart, R. L., Penna, J. L., et al. 2011, AJ, 141, 54

Anglada-Escudé, G., Boss, A. P., Weinberger, A. J., et al. 2012, ApJ, 746, 37

Artigau, É., Bouchard, S., Doyon, R., & Lafrenière, D. 2009, ApJ, 701, 1534

Artigau, É., Doyon, R., Lafrenière, D., et al. 2006, ApJ, 651, L57

Boller, T., Freyberg, M. J., Trümper, J., et al. 2016, A&A, 588, A103

Bonfils, X., Gillon, M., Udry, S., et al. 2012, A&A, 546, A27

Bonfils, X., Delfosse, X., Udry, S., et al. 2013, A&A, 549, 109

Boss, A. P., Weinberger, A. J., Anglada-Escudé, G., et al. 2009, PASP, 121, 1218

Bouy, H., Brandner, W., Martín, E. L., et al. 2003, AJ, 126, 1526

Bowler, B. P., Liu, M. C., & Dupuy, T. J. 2010, ApJ, 710, 45

Bowler, B. P., Liu, M. C., Shkolnik, E. L., & Tamura, M. 2015, ApJS, 216, 7

Burgasser, A. J., Reid, I. N., Leggett, S. K., et al. 2005, ApJ, 634, L177

Burgasser, A. J., Sitarski, B. N., Gelino, C. R., Logsdon, S. E., & Perrin, M. D. 2011, ApJ, 739, 49

Costa, E., Méndez, R. A., Jao, W.-C., et al. 2005, AJ, 130, 337

—. 2006, AJ, 132, 1234

Crifo, F., Phan-Bao, N., Delfosse, X., et al. 2005, A&A, 441, 653

Cruz, K. L., & Reid, I. N. 2002, AJ, 2828

Dahn, C. C., Harrington, R. S., Riepe, B. Y., et al. 1982, AJ, 87, 419

Dahn, C. C., Harrington, R. S., Kallarakal, V. V., et al. 1988, AJ, 95, 237

Dahn, C. C., Harris, H. C., Vrba, F. J., et al. 2002, AJ, 124, 1170

Deacon, N. R., & Hambly, N. C. 2001, A&A, 380, 148

—. 2007, A&A, 468, 163

Deacon, N. R., Hambly, N. C., & Cooke, J. A. 2005, A&A, 435, 363

Delfosse, X., Forveille, T., Ségransan, D., et al. 2000, A&A, 364, 217

Demory, B.-O., Torres, G., Neves, V., et al. 2013, ApJ, 768, 154

Dieterich, S. B., Henry, T. J., Jao, W.-C., et al. 2014, AJ, 147, 94

Dupuy, T. J., & Liu, M. C. 2012, ApJS, 201, 19

Faherty, J. K., Burgasser, A. J., Cruz, K. L., et al. 2009, AJ, 137, 1

Faherty, J. K., Burgasser, A. J., Walter, F. M., et al. 2012, ApJ, 752, 56

Faherty, J. K., Riedel, A. R., Cruz, K. L., et al. 2016, ApJ, submitted

Gagné, J., Faherty, J. K., Cruz, K. L., et al. 2015, ApJS, 219, 33

Gatewood, G. 2008, AJ, 136, 452

Gelino, C. R., Kulkarni, S. R., & Stephens, D. C. 2006, PASP, 118, 611

Harrington, R. S., & Dahn, C. C. 1980, AJ, 85, 454

Harrington, R. S., Dahn, C. C., Kallarakal, V. V., et al. 1993, Astronomical Journal (ISSN 0004-6256), 105, 1571

Hawley, S. L., Gizis, J. E., & Reid, I. N. 1996, Astronomical Journal v.112, 112, 2799

Heintz, W. D. 1994, AJ, 108, 2338

Henry, T. J., Jao, W.-C., Subasavage, J. P., et al. 2006, AJ, 132, 2360

Ianna, P. A., & Fredrick, L. W. 1995, ApJ, 441, L47

Jao, W.-C., Henry, T. J., Subasavage, J. P., et al. 2005, AJ, 129, 1954

—. 2011, AJ, 141, 117

Kendall, T. R., Jones, H. R. A., Pinfield, D. J., et al. 2007, MNRAS, 374, 445

Kervella, P., Thévenin, F., Di Folco, E., & Ségransan, D. 2004, A&A, 426, 297

Koerner, D. W., Kirkpatrick, J. D., McElwain, M. W., & Bonaventura, N. R. 1999, ApJ, 526, L25

Leinert, C., Weitzel, N., Richichi, A., Eckart, A., & Tacconi-Garman, L. E. 1994, A & A, 291, L47

Lodieu, N., Scholz, R.-D., McCaughrean, M. J., et al. 2005, A&A, 440, 1061

Malo, L., Artigau, É., Doyon, R., et al. 2014, ApJ, 788, 81

Malo, L., Doyon, R., Lafrenière, D., et al. 2013, ApJ, 762, 88

Mamajek, E. E., Bartlett, J. L., Seifahrt, A., et al. 2013, AJ, 146, 154

Marocco, F., Andrei, A. H., Smart, R. L., et al. 2013, AJ, 146, 161

Marshall, J. L. 2008, AJ, 135, 1000

McCaughrean, M. J., Close, L. M., Scholz, R.-D., et al. 2004, A&A, 413, 1029

Monet, D. G., Levine, S. E., Canzian, B., et al. 2003, AJ, 125, 984

Pecaut, M. J., & Mamajek, E. E. 2013, ApJS, 208, 9

Phan-Bao, N., & Bessell, M. S. 2006, A&A, 446, 515

Pope, B., Martinache, F., & Tuthill, P. 2013, ApJ, 767, 110

Pravdo, S. H., & Shaklan, S. B. 2009, ApJ, 700, 623

Reid, I. N., & Cruz, K. L. 2002, AJ, 123, 2806

Reid, I. N., Cruz, K. L., & Allen, P. R. 2007, AJ, 133, 2825

Reid, I. N., Cruz, K. L., Burgasser, A. J., & Liu, M. C. 2008, AJ, 135, 580

Reid, I. N., & Gizis, J. E. 2005, PASP, 117, 676

Reid, I. N., Hawley, S. L., & Gizis, J. E. 1995, AJ, 110, 1838

Reid, I. N., Cruz, K. L., Allen, P., et al. 2003, AJ, 126, 3007

Riaz, B., Gizis, J. E., & Harvin, J. 2006, AJ, 132, 866

Riedel, A. R., Murphy, S. J., Henry, T. J., et al. 2011, AJ, 142, 104

Riedel, A. R., Subasavage, J. P., Finch, C. T., et al. 2010, AJ, 140, 897

Riedel, A. R., Finch, C. T., Henry, T. J., et al. 2014, AJ, 147, 85

Sahlmann, J., Lazorenko, P. F., Ségransan, D., et al. 2014, A&A, 565, A20

Scholz, R.-D., Meusinger, H., & Jahreiß, H. 2005, A&A, 442, 211

Shkolnik, E., Liu, M. C., & Reid, I. N. 2009, ApJ, 699, 649

Skrutskie, M. F., Cutri, R. M., Stiening, R., et al. 2006, AJ, 131, 1163

Smart, R. L., Ioannidis, G., Jones, H. R. A., Bucciarelli, B., & Lattanzi, M. G. 2010, A&A, 514, 84

Tinney, C. G. 1996, MNRAS, 281, 644

Tinney, C. G., Reid, I. N., Gizis, J., & Mould, J. R. 1995, Astronomical Journal v.110, 110, 3014

van Altena, W. F., Lee, J. T., & Hoffleit, E. D. 1995, The general catalogue of trigonometric [stellar] parallaxes, 4th edn. (New Haven, CT: Yale University Observatory)

van Leeuwen, F. 2007, Springer

Vrba, F. J., Henden, A. A., Luginbuhl, C. B., et al. 2004, AJ, 127, 2948

Weinberger, A. J., Anglada-Escudé, G., & Boss, A. P. 2013, ApJ, 762, 118

Zapatero Osorio, M. R., Béjar, V. J. S., Miles-Páez, P. A., et al. 2014, A&A, 568, A6

This preprint was prepared with the AAS LaTeX macros v5.2.

Table 1. Observational information for CAPSCam targets with solved parallaxes

Name	RA hh mm ss.ss	Decl. dd mm ss.s	Sp. type	Ref	$t_{int,FF}$ (s)	$t_{int,GW}$ (s)	# ref ⋆s	# epochs	$Date_{start}$ (JD)	$Date_{end}$ (JD)	Δ t (yr)	m_J mag	σm_J mag	m_{W1} mag	σm_{W1} mag
GJ 1002	00 06 43.25	-07 32 14.7	M5.5	1	120	2	13	14	2455141.6	2456999.5	5.1	8.323	0.019	7.16	0.05
LEHPM 193	00 07 07.80	-24 58 03.8	M7	2	120	···	13	5	2455076.7	2456492.8	3.9	13.115	0.024	11.84	0.02
DY Psc	00 24 24.63	-01 58 20.1	M9.5	2	120	30	35	16	2454722.7	2456995.5	6.2	11.992	0.035	10.17	0.02
GJ 2005 A	00 24 44.18	-27 08 25.2	M5.5	1	120	5	22	5	2455410.9	2456587.7	3.2	9.254	0.034	7.81	0.02
LEHPM 1130	00 58 06.43	-53 18 09.2			120	···	20	5	2454347.8	2456491.8	5.9	12.998	0.024	11.73	0.02
GJ 1028	01 04 53.68	-18 07 29.3	M5	1	120	1	23	20	2454346.8	2456993.5	7.2	9.387	0.026	8.22	0.02
LP 647-13	01 09 51.17	-03 43 26.4	M9	2	120	20	17	10	2454290.9	2456488.9	6.0	11.694	0.021	10.08	0.02
LEHPM 1563	01 27 31.96	-31 40 03.2	M7	3	120	30	19	7	2454343.8	2456554.8	6.1	12.659	0.026	11.4	0.02
SIPS J013656	01 36 56.62	+09 33 47.3	T2.5	2	120	···	22	10	2456137.9	2457000.5	2.4	13.455	0.03	11.94	0.02
	01 39 21.71	-39 36 08.8			120	2	21	17	2455410.9	2456994.6	4.3	9.209	0.023	8.08	0.02
LHS 1295	01 46 22.62	-19 53 41.2			120	···	18	4	2455404.9	2455841.7	1.2	14.64	0.029	13.79	0.03
TZAri	02 00 12.96	+13 03 07.0	M4.5	1	120	0.2	16	14	2454814.6	2457000.6	6.0	7.514	0.017	6.46	0.08
GJ 3128	02 02 16.20	+10 20 13.7	M6	1	60	2	14	17	2454815.5	2457001.5	6.0	9.842	0.023	8.69	0.02
	02 05 29.40	-11 59 29.6	L7	2	120	···	18	14	2454719.8	2456995.6	6.2	14.587	0.03	12.23	0.02
LHS 1367	02 15 08.02	-30 40 01.2	M8	2	120	5	27	21	2454346.9	2456993.6	7.2	11.617	0.026	10.33	0.02
LP 649-93	02 18 57.92	-06 17 50.0	M8	2	60	···	32	4	2454347.8	2456552.8	6.0	12.85	0.024	11.59	0.02
	02 22 47.68	-27 32 34.9			120	15	29	14	2454344.9	2457001.6	7.3	12.053	0.024	10.84	0.02
GJ 3180	02 46 14.78	-04 59 18.2	M6	1	120	2	25	10	2454722.8	2457001.6	6.2	10.97	0.024	9.92	0.02
Teergarden's	02 53 00.84	+16 52 53.3	M7	2	60	2	24	17	2454815.6	2456999.6	6.0	8.394	0.027	7.14	0.05
	02 55 03.58	-47 00 51.0	L8	2	120	···	18	16	2455137.7	2457001.7	5.1	13.246	0.027	10.77	0.02
GJ 3198	03 04 04.52	-20 22 43.4	M3.5	1	60	1	17	11	2455515.7	2456995.6	4.1	8.634	0.023	7.55	0.03
CD Cet	03 13 22.99	+04 46 29.4	M5	1	60	0.5	17	14	2454724.8	2457000.6	6.2	8.775	0.02	7.6	0.03
LEHPM 3263	03 20 58.86	-55 20 15.8	M5.5	4	120	15	20	5	2454343.9	2455140.8	2.2	12.074	0.024	10.89	0.02
LP 888-18	03 31 30.25	-30 42 38.3	M7.5	2	120	10	20	11	2454345.9	2456994.6	7.3	11.36	0.022	10.07	0.02
	03 34 12.18	-49 53 32.3	M9	2	60	20	26	13	2454855.6	2457000.7	5.9	11.376	0.023	10.08	0.02
GJ 1061	03 35 59.69	-44 30 45.3	M5.5	5	120	0.4	18	18	2454348.9	2457001.8	7.3	7.523	0.02	6.39	0.09
LP 944-20	03 39 35.22	-35 25 44.1	M9	2	30	15	13	20	2454347.9	2456999.7	7.3	10.725	0.021	9.13	0.02
GJ 3252	03 51 00.47	-00 52 45.3	M7.5	2	120	···	12	4	2456615.8	2457040.5	1.2	11.302	0.024	9.97	0.02
LP 889-13	03 55 47.79	-27 09 08.3	M6.0	6	120	···	13	4	2455076.9	2455546.6	1.3	12.739	0.023	11.58	0.02
LP 833-40	04 06 52.37	-25 17 30.6	M6.0	6	120	30	18	4	2454816.6	2455219.5	1.1	12.714	0.028	11.55	0.02
	04 13 20.39	-01 14 24.9	L0.5	2	60	···	16	5	2455515.7	2455943.6	1.2	15.303	0.049	13.81	0.03
	04 23 48.58	-04 14 03.5	T0	2	120	···	23	13	2454720.9	2457039.5	6.3	14.465	0.027	12.18	0.02
GJ 3289	04 26 19.92	+03 36 35.9	M6.5	1	120	10	33	10	2454724.9	2457038.5	6.3	11.623	0.024	10.46	0.02
LP 775-31	04 35 16.13	-16 06 57.5	M7	2	60	5	28	13	2455515.7	2457037.6	4.2	10.406	0.026	9.1	0.02

Table 1—Continued

Name	RA hh mm ss.ss	Decl. dd mm ss.s	Sp. type	Ref	$t_{int,FF}$ (s)	$t_{int,GW}$ (s)	# ref ⋆s	# epochs	$Date_{start}$ (JD)	$Date_{end}$ (JD)	Δ t (yr)	m_J mag	σm_J mag	m_{W1} mag	σm_{W1} mag
LP 655-48	04 40 23.25	-05 30 08.3	M7	2	30	3	19	18	2454857.6	2457040.6	6.0	10.658	0.024	9.36	0.02
LP 776-7	04 44 46.18	-18 40 59.5	M6.0	6	120	30	21	5	2454816.7	2457082.5	6.2	13.034	0.027	11.82	0.02
LP 776-26	04 52 27.94	-19 54 46.2	M6.0	6	30	···	21	4	2454814.7	2456616.7	4.9	12.62	0.027	11.41	0.02
GJ 3323	05 01 57.46	-06 56 45.9	M4	1	60	0.2	22	16	2454814.6	2457037.6	6.1	7.617	0.032	6.55	0.08
	05 39 52.00	-00 59 01.9	L5	2	120	···	28	13	2454816.8	2457038.6	6.1	14.033	0.031	11.89	0.02
V1352 Ori	05 42 09.27	+12 29 21.6	M4	1	60	0.2	31	16	2454817.7	2457039.6	6.1	7.124	0.021	6.23	0.09
	05 59 19.14	-14 04 48.9	T5	2	120	···	29	17	2454161.5	2457040.6	7.9	13.802	0.024	13.39	0.03
G 99-49	06 00 03.49	+02 42 23.7	M4	1	60	0.2	36	16	2454819.7	2456993.8	6.0	6.905	0.02	6.01	0.09
LHS 1810	06 02 54.23	-09 15 03.1	M5.5	7	120	10	28	13	2454167.5	2457039.6	7.9	10.981	0.022	9.81	0.02
AP Col	06 04 52.16	-34 33 36.1	M5	8	60	0.2	22	18	2454814.7	2457037.7	6.1	7.742	0.027	6.67	0.07
	06 24 45.95	-45 21 54.9	L5	2	120	···	47	22	2454814.7	2457080.5	6.2	14.48	0.029	11.85	0.02
	06 41 18.40	-43 22 32.9	L1.5	2	60	···	26	19	2454166.5	2457039.7	7.9	13.751	0.026	12.1	0.02
G 108-21	06 42 11.19	+03 34 52.6	M3.5	1	60	1	27	7	2455297.5	2457038.7	4.8	8.166	0.021	7.15	0.04
G 108-22	06 42 13.34	+03 35 31.1	M4	1	60	1	25	8	2455219.7	2457040.7	5.0	9.112	0.027	8.1	0.02
Ruiz 207-61	07 07 53.28	-49 00 50.4	M8	2	60	···	33	6	2454814.8	2456705.6	5.2	13.228	0.026	11.85	0.02
GJ 3470	07 59 05.87	+15 23 29.5	M1.5	1	60	0.3	28	7	2456610.9	2457082.6	1.3	8.794	0.026	7.81	0.03
GJ 299	08 11 57.57	+08 46 22.0	M4.5	1	30	0.2	22	18	2454818.8	2457037.7	6.1	8.424	0.023	7.18	0.03
	08 32 04.52	-01 28 36.0	L1.5	2	120	···	24	5	2454166.6	2456694.7	6.9	14.128	0.03	12.42	0.02
V488 Hya	08 35 42.56	-08 19 23.8	L5	2	120	10	25	17	2454816.8	2457082.6	6.2	13.169	0.024	10.41	0.02
GJ 317	08 40 59.24	-23 27 23.3	M3.5	1	60	0.2	29	28	2454811.7	2457037.8	6.1	7.934	0.027	6.87	0.06
GJ 3517	08 53 36.19	-03 29 32.1	M9	2	60	10	22	17	2454166.7	2457039.7	7.9	11.212	0.026	9.62	0.02
GJ 1123	09 17 05.32	-77 49 23.4	M4.5	5	60	0.3	24	12	2455295.5	2457040.8	4.8	8.329	0.024	7.14	0.08
GJ 1128	09 42 46.35	-68 53 06.0	M4.5	5	60	0.2	31	14	2454817.8	2457038.8	6.1	7.953	0.024	6.82	0.03
GJ 1129	09 44 47.31	-18 12 48.9	M4	1	20	0.2	33	10	2455296.5	2457039.8	4.8	8.122	0.026	6.97	0.05
G 161-71	09 44 54.22	-12 20 54.4	M5	8	60	0.3	28	11	2455295.5	2457038.8	4.8	8.496	0.024	7.36	0.03
GJ 3618	10 44 21.32	-61 12 38.4	M5.5	9	60	2	57	14	2454851.8	2457037.8	6.0	8.492	0.021	7.46	0.03
GJ 3622	10 48 12.58	-11 20 08.2	M6.5	1	60	1	23	13	2454852.8	2457037.9	6.0	8.857	0.021	7.66	0.03
	10 48 14.64	-39 56 06.2	M9	2	120	5	29	17	2454161.5	2457038.9	7.9	9.538	0.022	8.08	0.02
EE Leo	10 50 52.03	+06 48 29.2	M4	1	120	0.3	12	10	2454853.8	2457040.8	6.0	7.319	0.023	6.28	0.1
CN Leo	10 56 28.86	+07 00 52.8	M5.5	1	30	0.2	12	13	2454810.9	2457039.8	6.1	7.085	0.024	5.84	0.14
	10 58 47.87	-15 48 17.2	L3	2	120	···	29	10	2454166.7	2456767.6	7.1	14.155	0.035	12.08	0.02
	11 26 39.91	-50 03 55.0	L9	2	60	···	50	8	2455546.9	2456765.6	3.3	13.997	0.032	12.22	0.02
GJ 3668	11 31 08.36	-14 57 20.2	M4.5	1	120	1	27	9	2454855.8	2456768.6	5.2	9.359	0.026	8.23	0.02
GJ 452.1	11 54 07.91	+09 48 22.8	M3.5	1	60	0.4	16	7	2455296.7	2456767.6	4.0	8.699	0.03	7.63	0.03

Table 1—Continued

Name	RA hh mm ss.ss	Decl. dd mm ss.s	Sp. type	Ref	$t_{int,FF}$ (s)	$t_{int,GW}$ (s)	# ref ⋆s	# epochs	$Date_{start}$ (JD)	$Date_{end}$ (JD)	Δ t (yr)	m_J mag	σm_J mag	m_{W1} mag	σm_{W1} mag
	11 55 39.52	-37 27 35.1	L2	2	120	30	31	13	2454161.5	2456767.7	7.1	12.811	0.024	11.04	0.02
LP 851-346	11 55 42.86	-22 24 58.6	M7.5	2	120	10	25	5	2455218.9	2456766.6	4.2	10.93	0.023	9.66	0.02
GJ 1154	12 14 16.54	+00 37 26.4	M5	1	120	1	12	4	2454854.8	2456764.6	5.2	8.456	0.026	7.24	0.04
GL Vir	12 18 59.39	+11 07 33.9	M5	1	60	0.5	29	7	2454855.9	2456803.5	5.3	8.525	0.027	7.26	0.04
GJ 3737	12 38 49.14	-38 22 52.8	M4.5	5	120	0.5	30	9	2454856.8	2456765.6	5.2	8.174	0.024	7.16	0.04
	12 59 04.71	-43 36 24.4			60	5	37	17	2454813.9	2457080.9	6.2	10.534	0.022	9.23	0.02
FN Vir	13 00 33.50	+05 41 08.1	M4.5	1	120	0.5	12	9	2454666.5	2456766.7	5.7	8.553	0.035	7.41	0.03
Kelu-1	13 05 40.19	-25 41 06.0	L2	2	240	···	29	8	2454162.5	2456767.7	7.1	13.414	0.026	11.25	0.02
CE 303	13 09 21.85	-23 30 35.0	M8	2	90	6	29	6	2455296.7	2456764.7	4.0	11.785	0.022	10.44	0.02
	13 15 30.94	-26 49 51.3	L5.5	2	120	···	28	16	2454161.5	2456764.7	7.1	15.195	0.051	12.74	0.02
	14 09 03.10	-33 57 56.6	L2	2	240	···	35	5	2454162.5	2457080.9	8.0	14.248	0.026	12.54	0.02
	14 16 24.08	+13 48 26.3	L6	10	120	···	8	6	2456026.8	2457082.8	2.9	13.148	0.025	11.36	0.02
G 124-62B	14 41 37.17	-09 45 59.0	L0.5	2	120	···	21	4	2454162.5	2454984.6	2.3	14.02	0.029	12.34	0.02
LHS 3003	14 56 38.31	-28 09 47.4	M7	2	120	2	28	13	2454665.6	2456855.5	6.0	9.965	0.026	8.72	0.02
GJ 570 D	14 57 14.96	-21 21 47.8	T7	2	120	···	35	4	2454165.9	2454985.7	2.2	15.324	0.048	14.93	0.04
LP 859-1	15 04 16.22	-23 55 56.4	M7.5	2	30	···	30	4	2454166.9	2455373.6	3.3	12.011	0.026	10.79	0.02
	15 07 47.69	-16 27 38.6	L5	2	120	···	24	16	2454164.9	2456856.5	7.4	12.83	0.027	10.67	0.02
GJ 3900	15 19 11.82	-12 45 06.2	M4	1	42	0.2	38	7	2455297.7	2456855.5	4.3	8.507	0.026	7.42	0.03
2MUCD 11346	15 34 57.04	-14 18 48.7	M7	2	60	10	46	9	2455297.8	2456766.7	4.0	11.38	0.023	10.04	0.02
GJ 590	15 36 34.50	-37 54 22.3	M4.5	5	120	1	39	9	2455373.7	2456890.5	4.2	8.44	0.024	7.49	0.03
	15 39 41.90	-05 20 42.8	L4	2	120	···	32	6	2455375.6	2456855.6	4.1	13.922	0.029	12.01	0.02
LHS 5303	15 52 44.60	-26 23 13.4	M6	11	60	10	35	9	2455664.8	2456889.5	3.4	10.258	0.021	9.13	0.02
	15 55 15.73	-09 56 05.5	L1	2	60	···	24	9	2454986.7	2456888.5	5.2	12.557	0.024	11.14	0.04
	16 18 45.04	-13 21 29.8	L0	2	120	···	26	4	2454661.5	2455403.5	2.0	14.247	0.024	12.56	0.02
	16 19 28.31	+00 50 11.8	L2	2	120	···	21	7	2454986.7	2456138.6	3.2	14.391	0.036	12.74	0.02
GJ 3967	16 40 06.00	+00 42 18.8	M4	1	120	0.5	35	14	2454666.7	2456885.5	6.1	9.116	0.037	8.07	0.02
	16 45 22.11	-13 19 51.7	L1.5	2	60	···	33	19	2454284.7	2456886.5	7.1	12.451	0.028	10.8	0.02
GJ 644 C	16 55 35.29	-08 23 40.1	M7	1	120	5	25	17	2454665.7	2456889.6	6.1	9.776	0.029	8.62	0.02
GJ 1214	17 15 18.94	+04 57 49.7	M4.5	1	45	5	29	15	2455368.8	2456888.6	4.2	9.75	0.024	8.6	0.02
	17 50 24.84	-00 16 15.1	L5.5	2	60	···	32	11	2455667.8	2456885.5	3.3	13.294	0.023	11.18	0.02
GJ 1224	18 07 32.92	-15 57 46.5	M4.5	1	60	0.5	30	18	2454347.5	2456886.5	7.0	8.639	0.024	7.48	0.03
L 43-72	18 11 15.29	-78 59 22.7	M4.5	8	60	2	21	6	2455376.7	2455786.7	1.1	7.84	0.019	6.78	0.07
V816 Her	18 42 44.99	+13 54 16.8	M4	1	60	2	35	10	2455376.7	2456887.6	4.1	8.361	0.018	7.34	0.04
SCRJ1845-6357	18 45 05.41	-63 57 47.6	M8.5	2	60	5	29	26	2454928.9	2456885.6	5.4	9.544	0.023	8.15	0.02

Table 1—Continued

Name	RA hh mm ss.ss	Decl. dd mm ss.s	Sp. type	Ref	$t_{int,FF}$ (s)	$t_{int,GW}$ (s)	# ref ⋆s	# epochs	$Date_{start}$ (JD)	$Date_{end}$ (JD)	Δ t (yr)	m_J mag	σm_J mag	m_{W1} mag	σm_{W1} mag
GJ 4074	18 45 57.99	-28 54 53.1	M4	1	30	1	28	4	2455369.8	2456136.7	2.1	9.84	0.023	9.34	0.02
VB 10	19 16 57.62	+05 09 02.2	M8	2	60	5	16	6	2454932.9	2455405.6	1.3	9.908	0.025	8.53	0.02
GJ 754	19 20 47.95	-45 33 28.3	M4.5	5	60	0.2	27	21	2454345.6	2456886.6	7.0	7.661	0.019	6.69	0.06
GJ 1236	19 22 02.07	+07 02 31.0	M3	1	30	3	39	10	2455410.7	2456888.6	4.0	8.524	0.026	7.51	0.03
LP 869-19	19 42 00.65	-21 04 05.2	M3.5	8	30	1	39	12	2455366.8	2456887.6	4.2	8.692	0.019	7.61	0.03
LP 870-65	20 04 30.78	-23 42 01.9	M4	8	60	1	33	14	2455368.9	2456885.6	4.2	8.559	0.027	7.5	0.03
LP 695-72	20 24 15.04	-04 15 32.1			120	30	30	6	2454347.6	2456552.6	6.0	12.201	0.026	11.15	0.02
GJ 1251	20 28 03.83	-76 40 16.4	M4.5	5	120	2	30	17	2454348.6	2456886.6	6.9	9.359	0.022	8.43	0.02
	20 28 20.35	+00 52 26.6	L3	2	120	···	31	4	2454344.6	2455078.6	2.0	14.298	0.035	12.3	0.02
LHS 3566	20 39 23.79	-29 26 33.6	M5.5	12	60	10	26	14	2454346.6	2456889.6	7.0	11.357	0.025	10.17	0.02
GJ 1256	20 40 33.64	+15 29 57.2	M4.5	1	60	0.6	30	12	2454989.9	2456888.7	5.2	8.641	0.027	7.5	0.03
GJ 810 B	20 55 37.07	-14 03 54.6	M5	5	60	3	25	14	2454348.6	2456889.6	7.0	9.717	0.024	8.76	0.02
GJ 810A	20 55 37.72	-14 02 07.8	M4	5	60	0.5	26	13	2454348.7	2456885.7	6.9	8.117	0.027	7.12	0.04
	20 57 54.09	-02 52 30.3	L1.5	2	60	···	28	20	2454284.8	2456887.7	7.1	13.121	0.024	11.29	0.02
	21 04 14.91	-10 37 37.0	L3	2	120	···	25	12	2454719.6	2456886.7	5.9	13.841	0.029	11.91	0.02
LHS 504	21 05 14.06	-24 46 50.4	sdM4.5	13	30	···	24	7	2454291.8	2455407.8	3.1	13.355	0.033	12.46	0.02
LP 759-17	22 02 11.25	-11 09 46.1	M6.5	11	120	30	12	5	2454345.7	2455076.7	2.0	12.361	0.024	11.1	0.02
Eps Indi B	22 04 10.52	-56 46 57.7	T1+T6	2	60	···	28	19	2454286.8	2456887.7	7.1	11.908	0.022	···	···
GJ 1265	22 13 42.78	-17 41 08.2	M4.5	1	45	1	24	15	2455369.8	2456888.7	4.2	8.955	0.029	7.97	0.02
GJ 4274	22 23 06.97	-17 36 25.0	M4.5	1	60	0.3	29	18	2454991.9	2456885.7	5.2	8.242	0.027	7.01	0.04
	22 24 43.81	-01 58 52.1	L4.5	2	120	···	23	15	2454346.7	2456886.7	7.0	14.073	0.027	11.41	0.02
GJ 4281	22 28 54.40	-13 25 17.9	M6.5	1	120	10	20	16	2454347.7	2456889.7	7.0	10.768	0.023	9.68	0.02
LP 876-10	22 48 04.47	-24 22 07.5	M4	14	60	0.5	24	13	2455368.9	2456890.7	4.2	8.075	0.023	6.92	0.05
LHS 3872	22 54 46.49	-05 28 26.2	M4.5	1	120	5	24	7	2454720.7	2455837.6	3.1	9.65	0.023	8.6	0.02
GL 877	22 55 45.51	-75 27 31.2	M2.5	5	60	0.4	19	6	2455076.7	2455840.6	2.1	6.616	0.018	5.72	0.13
	23 06 29.28	-05 02 28.6	M8	2	90	10	19	11	2455787.8	2456888.7	3.0	11.354	0.022	10.07	0.02
LHS 3970	23 33 40.57	-21 33 52.6	M5.0	11	60	10	6	6	2454665.8	2455404.8	2.0	11.858	0.021	10.77	0.02
GJ 1286	23 35 10.50	-02 23 21.4	M5.5	1	120	5	16	22	2454346.7	2456886.8	7.0	9.148	0.021	7.97	0.02
GJ 4350	23 36 52.27	-36 28 51.8	M4.5	5	120	2	12	19	2454348.7	2456887.8	7.0	9.191	0.037	8.21	0.02
LHS 3992	23 39 18.89	-20 56 55.8			60	···	23	9	2454285.9	2455842.7	4.3	14.555	0.03	13.79	0.03
LEHPM 6494	23 56 10.81	-34 26 04.4	M9.0	15	60	···	22	19	2454662.9	2456885.8	6.1	12.947	0.024	11.63	0.02
LP 880-140	23 59 03.89	-29 32 22.7	M6.5	16	120	10	7	7	2454286.9	2455409.8	3.1	12.384	0.026	11.28	0.02

Note. — Spectral types are visual wavelength where available. J magnitudes are from 2MASS, W1 magnitudes are from ALLWISE.
(Table 1 will be published online in its entirety in a machine readable format. The published paper will show a stub table for guidance regarding its form and content.)

References. — [1] Reid et al. (1995); [2] Faherty et al. (2009); [3] Kendall et al. (2007); [4] Phan-Bao & Bessell (2006); [5] Hawley et al. (1996); [6] Cruz & Reid (2002); [7] Reid et al. (2003); [8] Riaz et al. (2006); [9] Bonfils et al. (2013); [10] Bowler et al. (2010); [11] Crifo et al. (2005); [12] Reid & Gizis (2005); [13] Marshall (2008); [14] Scholz et al. (2005); [15] Lodieu et al. (2005); [16] Reid et al. (2007)

Table 2. Astrometric Results

Name	RA	Decl.	$\pi_{\rm rel}$ (mas)	$\sigma\pi_{\rm rel}$ (mas)	Zero Pt (mas)	$\sigma_{\rm ZPt}$ (mas)	$\pi_{\rm Lit.}$ (mas)	$\sigma\pi_{\rm Lit}$ (mas)	Ref	μ_{RA} ($cos\delta$,rel) (mas yr^{-1})	$\sigma\mu$ ($cos\delta$,rel) (mas yr^{-1})	μ_{δ} (rel) (mas yr^{-1})	$\sigma\mu$ (rel) (mas yr^{-1})	$\pi_{\rm abs}$ (mas)	$\sigma\pi_{\rm abs}$ (mas)
GJ 1002	00 06 43.25	-07 32 14.7	206.92	0.97	-0.50	0.75	213	3.6	1	-805.16	0.56	-1870.61	0.37	207.42	1.23
LEHPM 193	00 07 07.80	-24 58 03.8	38.80	1.27	0.00	0.40				184.84	0.66	-56.55	0.52	38.80	1.33
DY Psc	00 24 24.63	-01 58 20.1	79.78	0.91	-0.93	0.26	84.3	2.6	1,2	-78.23	0.30	141.47	0.60	80.71	0.95
GJ 2005 A	00 24 44.18	-27 08 25.2	123.97	11.40	-8.33	0.03	129.7	2.4	1,3	-106.57	5.72	690.64	7.83	132.3	11.4
LEHPM 1130	00 58 06.43	-53 18 09.2	28.39	0.97	0.00	0.40				-202.64	0.43	-237.61	0.22	28.39	1.05
GJ 1028	01 04 53.68	-18 07 29.3	101.43	0.43	-0.80	0.75	99.80	5.00	1	1274.41	0.12	494.08	0.35	102.23	0.86
LP 647-13	01 09 51.17	-03 43 26.4	98.32	1.30	0.77	1.58	104.23	2.29	3	365.34	0.42	15.57	0.42	97.55	2.04
LEHPM 1563	01 27 31.96	-31 40 03.2	38.22	3.89	-1.49	0.87				284.10	1.48	137.70	8.91	39.71	3.99
SIPS J013656	01 36 56.62	+09 33 47.3	162.32	0.89	-0.56	0.40				1222.70	0.78	0.54	1.23	162.88	0.98
	01 39 21.71	-39 36 08.8	112.98	0.37	-0.71	0.40				133.74	0.18	-219.96	0.34	113.69	0.54
LHS 1295	01 46 22.62	-19 53 41.2	10.03	0.86	-0.66	0.40				-129.50	1.09	-640.46	2.93	10.69	0.95
TZAri	02 00 12.96	+13 03 07.0	220.84	0.49	-0.83	0.52	222	5	4	1093.29	0.20	-1745.18	0.52	221.67	0.71
GJ 3128	02 02 16.20	+10 20 13.7	108.46	0.41	-0.28	0.40	112	1.9	1,5	-670.58	0.18	-274.75	0.34	108.74	0.57
	02 05 29.40	-11 59 29.6	54.86	1.13	0.58	1.13	50.6	1.5	6	427.97	0.44	56.17	0.50	54.28	1.59
LHS 1367	02 15 08.02	-30 40 01.2	70.69	1.01	0.43	0.71				761.53	0.37	-348.99	0.29	70.26	1.23
LP 649-93	02 18 57.92	-06 17 50.0	34.05	0.45	0.71	0.40				342.33	0.13	-86.01	0.53	33.34	0.60
	02 22 47.68	-27 32 34.9	58.59	0.34	0.00	0.40				-198.36	0.10	-129.65	0.16	58.59	0.52
GJ 3180	02 46 14.78	-04 59 18.2	59.36	0.66	-0.74	0.63	61	8.2	7	1676.06	0.27	-1856.16	0.16	60.10	0.91
Teergarden's	02 53 00.84	+16 52 53.3	259.60	0.61	-0.65	0.71	259.3	0.9	8	3414.92	0.25	-3749.90	0.24	260.25	0.93
	02 55 03.58	-47 00 51.0	205.83	0.35	0.00	0.40	201.37	3.89	9	999.09	0.45	-547.61	0.13	205.83	0.53
GJ 3198	03 04 04.52	-20 22 43.4	56.57	0.58	-0.66	1.33	67.28	1.25	10	480.02	0.27	-474.92	0.59	57.23	1.45
CD Cet	03 13 22.99	+04 46 29.4	116.82	0.71	0.88	0.40	117.1	3.5	1	1718.44	0.26	104.43	0.35	115.94	0.81
LEHPM 3263	03 20 58.86	-55 20 15.8	45.71	0.95	0.02	1.12				293.39	0.74	267.34	1.57	45.69	1.47
LP 888-18	03 31 30.25	-30 42 38.3	80.74	0.50	1.75	0.98				46.81	0.16	-395.81	0.14	78.99	1.10
	03 34 12.18	-49 53 32.3	111.29	0.70	0.00	0.40	120.6	3.6	11	2335.68	0.27	486.33	0.64	111.29	0.81
GJ 1061	03 35 59.69	-44 30 45.3	269.25	0.59	0.59	0.01	271.9	1.34	8	733.93	0.24	-368.69	0.33	268.66	0.59
LP 944-20	03 39 35.22	-35 25 44.1	154.09	0.53	-0.35	0.29	158.5	1	12,13	297.91	0.17	266.89	0.70	154.44	0.60
GJ 3252	03 51 00.47	-00 52 45.3	73.06	1.79	0.96	1.82	68.10	1.80	1	22.12	1.83	-460.26	5.10	72.10	2.55
LP 889-13	03 55 47.79	-27 09 08.3	30.21	2.19	0.31	0.37				378.68	2.95	6.96	4.61	29.90	2.22
LP 833-40	04 06 52.37	-25 17 30.6	31.63	1.43	0.14	1.42				402.53	1.54	182.95	1.26	31.50	2.02
	04 13 20.39	-01 14 24.9	15.21	0.72	-0.13	0.18				67.12	1.16	-10.06	1.81	15.34	0.74
	04 23 48.58	-04 14 03.5	67.25	2.28	-0.22	0.10	65.93	1.7	14	-321.03	1.01	82.04	0.64	67.47	2.28

Table 2—Continued

Name	RA	Decl.	$\pi_{\rm rel}$ (mas)	$\sigma\pi_{\rm rel}$ (mas)	Zero Pt (mas)	$\sigma_{\rm ZPt}$ (mas)	$\pi_{\rm Lit.}$ (mas)	$\sigma\pi_{\rm Lit}$ (mas)	Ref	μ_{RA} ($cos\delta$,rel) (mas yr^{-1})	$\sigma\mu$ ($cos\delta$,rel) (mas yr^{-1})	μ_{δ} (rel) (mas yr^{-1})	$\sigma\mu$ (rel) (mas yr^{-1})	$\pi_{\rm abs}$ (mas)	$\sigma\pi_{\rm abs}$ (mas)
GJ 3289	04 26 19.92	+03 36 35.9	64.35	1.41	-0.89	0.55	58.4	1.8	1	-119.02	0.33	-1001.15	0.43	65.24	1.51
LP 775-31	04 35 16.13	-16 06 57.5	95.66	1.64	0.07	0.65	95.35	1.06	13	155.78	0.80	313.33	0.87	95.59	1.76
LP 655-48	04 40 23.25	-05 30 08.3	101.93	0.99	-0.37	0.25	102.61	0.71	15	326.29	0.37	130.15	0.30	102.30	1.02
LP 776-7	04 44 46.18	-18 40 59.5	30.12	0.97	2.09	2.21				-6.61	0.31	-394.24	2.10	28.03	2.42
LP 776-26	04 52 27.94	-19 54 46.2	33.24	1.30	6.78	1.12				168.32	0.39	-270.10	0.44	26.46	1.72
GJ 3323	05 01 57.46	-06 56 45.9	183.98	0.90	0.08	0.28	187.9	1.26	8	-547.61	0.27	-529.89	0.46	183.91	0.94
	05 39 52.00	-00 59 01.9	78.90	0.98	-0.28	0.35	79.1	2.4	16	157.77	0.26	322.34	0.13	79.18	1.04
V1352 Ori	05 42 09.27	+12 29 21.6	171.49	0.83	-0.07	0.19	171.7	1.1	17	1984.77	0.25	-1548.34	0.82	171.56	0.85
	05 59 19.14	-14 04 48.9	96.76	1.20	-0.04	0.08	97.7	1.3	6	567.58	0.39	-332.07	0.18	96.80	1.20
G 99-49	06 00 03.49	+02 42 23.7	191.07	1.19	-0.33	0.23	189.9	1.8	1,8	305.76	0.45	-36.89	0.94	191.40	1.21
LHS 1810	06 02 54.23	-09 15 03.1	65.69	0.73	-0.12	0.14				116.70	0.16	-589.08	0.20	65.81	0.74
AP Col	06 04 52.16	-34 33 36.1	114.08	0.39	0.03	0.16	119.21	0.98	18	23.22	0.12	339.80	0.32	114.05	0.42
	06 24 45.95	-45 21 54.9	81.36	0.39	0.12	0.21	83.9	4.5	11	-37.15	0.15	370.45	0.13	81.24	0.44
	06 41 18.40	-43 22 32.9	50.54	0.50	-0.54	0.11	55.7	5.7	19	208.20	0.15	623.68	0.18	51.08	0.51
G 108-21	06 42 11.19	+03 34 52.6	64.04	0.57	-0.90	0.22	73	5.7	20	44.37	0.20	-256.45	2.31	64.94	0.61
G 108-22	06 42 13.34	+03 35 31.1	65.92	1.69	-0.56	0.26				46.61	0.43	-251.03	0.71	66.48	1.71
Ruiz 207-61	07 07 53.28	-49 00 50.4	41.01	1.62	0.03	0.20	54.7	2	1,21,12	-16.32	0.42	388.40	0.73	40.98	1.63
GJ 3470	07 59 05.87	+15 23 29.5	34.92	0.48	0.77	0.45				-181.95	0.81	-54.37	1.09	34.15	0.66
GJ 299	08 11 57.57	+08 46 22.0	147.16	0.36	0.03	0.28				1077.08	0.15	-5044.98	0.23	147.13	0.45
	08 32 04.52	-01 28 36.0	41.94	1.79	1.50	0.39	40	2.9	1	63.05	0.29	10.14	0.72	40.44	1.83
V488 Hya	08 35 42.56	-08 19 23.8	137.22	0.35	-0.27	0.16	117.3	11.2	19	-527.88	0.11	298.20	0.14	137.49	0.39
GJ 317	08 40 59.24	-23 27 23.3	65.60	0.54	-0.34	0.10	65.3	0.4	22	-458.02	0.19	794.61	0.25	65.94	0.55
GJ 3517	08 53 36.19	-03 29 32.1	114.47	1.01	-0.45	0.11	117.7	0.7	1,23,13	-507.25	0.32	-197.65	0.36	114.92	1.02
GJ 1123	09 17 05.32	-77 49 23.4	106.89	0.91	0.00	0.40	110.9	2	24	636.70	0.34	-803.57	0.49	106.89	0.99
GJ 1128	09 42 46.35	-68 53 06.0	152.57	0.50	-0.29	0.15	153.1	2.4	24	-70.83	0.21	1115.13	0.60	152.86	0.52
GJ 1129	09 44 47.31	-18 12 48.9	90.68	0.64	-0.46	0.27	93.9	2.5	25	-1580.87	0.24	-174.11	0.61	91.14	0.70
G 161-71	09 44 54.22	-12 20 54.4	74.90	0.82	-0.49	0.21				-323.17	0.33	40.24	0.30	75.39	0.85
GJ 3618	10 44 21.32	-61 12 38.4	205.53	0.75	-0.51	0.31	209.0	1.7	8	-342.21	0.26	1594.92	0.47	206.04	0.81
GJ 3622	10 48 12.58	-11 20 08.2	217.96	0.54	-0.14	0.26	220.3	3.6	1	88.59	0.21	-1513.45	0.32	218.10	0.60
	10 48 14.64	-39 56 06.2	246.05	0.59	-0.31	0.13	248.6	1.2	26,3,24	-1159.36	0.24	-986.08	0.31	246.36	0.60
EE Leo	10 50 52.03	+06 48 29.2	143.95	0.90	-0.17	0.19	147.9	3.5	27	-840.43	0.29	-809.96	1.10	144.12	0.92
CN Leo	10 56 28.86	+07 00 52.8	412.46	1.14	-0.67	0.56	418.90	2.40	28	-3808.09	0.30	-2692.61	0.42	413.13	1.27

Table 2—Continued

Name	RA	Decl.	$\pi_{\rm rel}$ (mas)	$\sigma\pi_{\rm rel}$ (mas)	Zero Pt (mas)	$\sigma_{\rm ZPt}$ (mas)	$\pi_{\rm Lit.}$ (mas)	$\sigma\pi_{\rm Lit}$ (mas)	Ref	μ_{RA} ($cos\delta$,rel) (mas yr^{-1})	$\sigma\mu$ ($cos\delta$,rel) (mas yr^{-1})	μ_{δ} (rel) (mas yr^{-1})	$\sigma\mu$ (rel) (mas yr^{-1})	$\pi_{\rm abs}$ (mas)	$\sigma\pi_{\rm abs}$ (mas)
	10 58 47.87	-15 48 17.2	55.83	0.39	-0.05	0.41	66.5	4.4	11	-250.39	0.12	32.41	0.11	55.88	0.56
	11 26 39.91	-50 03 55.0	60.81	1.92	0.00	0.40	59.38	1.64	13	-1571.93	1.49	440.06	0.31	60.81	1.96
GJ 3668	11 31 08.36	-14 57 20.2	86.95	0.43	0.80	0.30	89.2	1.7	24	415.97	0.19	-1359.45	0.39	86.15	0.53
GJ 452.1	11 54 07.91	+09 48 22.8	86.59	0.83	0.00	0.40	96.1	22.2	1	92.44	0.36	-790.04	0.68	86.59	0.92
	11 55 39.52	-37 27 35.1	84.00	0.76	-0.36	0.37	104.4	4.7	11	53.74	0.19	-784.49	0.27	84.36	0.85
LP 851-346	11 55 42.86	-22 24 58.6	90.72	0.50	-0.41	0.29	89.54	1.77	13	-363.48	0.22	-185.77	0.48	91.13	0.58
GJ 1154	12 14 16.54	+00 37 26.4	140.43	1.30	0.87	2.00	119.4	3.5	1	-936.97	0.72	-281.87	0.15	139.56	2.39
GL Vir	12 18 59.39	+11 07 33.9	154.43	0.80	-0.83	0.65	152.9	3	1	-1253.85	0.36	201.89	1.33	155.26	1.03
GJ 3737	12 38 49.14	-38 22 52.8	150.39	0.60	0.69	0.31	156.8	2	8	-646.09	0.26	-1303.80	0.39	149.70	0.68
	12 59 04.71	-43 36 24.4	128.79	1.22	-0.32	0.24	276	41	29	1101.54	1.20	-253.28	0.30	129.11	1.24
FN Vir	13 00 33.50	+05 41 08.1	119.79	2.46	0.00	0.00	123.1	3.5	1	-926.90	0.75	226.85	0.53	119.79	2.46
Kelu-1	13 05 40.19	-25 41 06.0	51.63	1.06	-0.12	0.47	53.6	2	6	-298.89	0.29	-9.29	0.36	51.75	1.16
CE 303	13 09 21.85	-23 30 35.0	69.10	1.42	-0.27	0.58	69.33	1.33	13	24.38	0.54	-377.82	0.71	69.37	1.53
	13 15 30.94	-26 49 51.3	52.02	1.18	-0.10	0.23				-675.52	0.33	-289.11	0.42	52.12	1.20
	14 09 03.10	-33 57 56.6	40.85	0.46	0.76	0.28				93.85	0.12	46.20	0.39	40.09	0.54
	14 16 24.08	+13 48 26.3	112.85	4.75	1.70	1.52	109.7	1.3	30	91.27	3.90	132.52	1.34	111.15	4.99
G 124-62B	14 41 37.17	-09 45 59.0	29.96	0.65	-0.70	0.29	36.4	3.6	9	-198.91	0.80	-19.60	1.01	30.66	0.71
LHS 3003	14 56 38.31	-28 09 47.4	140.50	0.52	-0.08	0.14	148.8	2.9	3,12	-476.91	0.19	-835.70	0.26	140.58	0.54
GJ 570 D	14 57 14.96	-21 21 47.8	167.56	4.58	0.00	0.40	171.22	0.94	27	1038.08	4.34	-1677.69	3.57	167.56	4.60
LP 859-1	15 04 16.22	-23 55 56.4	48.34	1.20	0.57	0.65				-322.50	0.82	-86.74	0.65	47.77	1.36
	15 07 47.69	-16 27 38.6	133.77	0.57	-0.16	0.09	136.4	0.6	6	-142.42	0.17	-886.09	0.16	133.93	0.58
GJ 3900	15 19 11.82	-12 45 06.2	47.24	3.63	-0.10	0.56				-704.23	1.35	-186.87	0.95	47.34	3.67
2MUCD 11346	15 34 57.04	-14 18 48.7	91.21	0.61	-0.02	0.15				-904.89	0.31	-327.29	0.41	91.23	0.63
GJ 590	15 36 34.50	-37 54 22.3	97.88	0.52	-0.69	0.12	81.6	13.7	1	-327.72	0.24	-794.68	0.41	98.57	0.53
	15 39 41.90	-05 20 42.8	59.88	1.15	-0.20	0.50	61.25	1.26	13	589.96	0.56	113.00	0.84	60.08	1.25
LHS 5303	15 52 44.60	-26 23 13.4	94.09	0.65	-0.55	0.07	94.63	0.7	13	215.39	0.51	-443.83	0.57	94.64	0.65
	15 55 15.73	-09 56 05.5	73.24	0.78	0.55	0.35	74.53	1.21	13	933.54	0.31	-767.07	0.20	72.69	0.85
	16 18 45.04	-13 21 29.8	22.56	1.04	0.70	0.75				-108.89	0.38	-79.77	1.17	21.86	1.28
	16 19 28.31	+00 50 11.8	39.47	4.21	-0.18	0.24				60.20	3.24	-72.67	1.43	39.65	4.22
GJ 3967	16 40 06.00	+00 42 18.8	89.10	0.69	-0.21	0.10	89	2.3	1	176.69	0.25	-149.88	0.31	89.31	0.70
	16 45 22.11	-13 19 51.7	88.55	0.39	-0.75	0.11	90.12	0.82	13	-351.89	0.11	-797.16	0.14	89.30	0.41
GJ 644 C	16 55 35.29	-08 23 40.1	153.75	0.50	-0.47	0.13	154.8	0.6	1	-796.20	0.20	-864.46	0.31	154.22	0.52

Table 2—Continued

Name	RA	Decl.	$\pi_{\rm rel}$ (mas)	$\sigma\pi_{\rm rel}$ (mas)	Zero Pt (mas)	$\sigma_{\rm ZPt}$ (mas)	$\pi_{\rm Lit.}$ (mas)	$\sigma\pi_{\rm Lit}$ (mas)	Ref	μ_{RA} ($cos\delta$,rel) (mas yr^{-1})	$\sigma\mu$ ($cos\delta$,rel) (mas yr^{-1})	μ_{δ} (rel) (mas yr^{-1})	$\sigma\mu$ (rel) (mas yr^{-1})	$\pi_{\rm abs}$ (mas)	$\sigma\pi_{\rm abs}$ (mas)
GJ 1214	17 15 18.94	+04 57 49.7	67.75	0.41	-0.52	0.16	77.2	5.4	1	581.11	0.24	-733.62	0.48	68.27	0.44
	17 50 24.84	-00 16 15.1	108.31	0.82	-0.47	0.15				-394.73	0.55	197.10	0.62	108.78	0.83
GJ 1224	18 07 32.92	-15 57 46.5	123.51	0.77	0.00	0.40	127	1	1,15	-610.57	0.28	-341.31	0.36	123.51	0.87
L 43-72	18 11 15.29	-78 59 22.7	83.46	3.63	1.13	0.58				39.55	5.92	-126.98	6.71	82.33	3.68
V816 Her	18 42 44.99	+13 54 16.8	91.34	0.66	-0.33	0.48	90.2	1.9	1,15	-31.16	0.37	355.14	0.48	91.67	0.82
SCRJ1845-6357	18 45 05.41	-63 57 47.6	246.59	1.33	0.00	0.40	259.5	1.1	29,8	2567.02	0.49	610.29	0.40	246.59	1.39
GJ 4074	18 45 57.99	-28 54 53.1	9.47	0.58	0.00	0.40				8.71	0.26	-126.98	0.39	9.47	0.70
VB 10	19 16 57.62	+05 09 02.2	168.15	0.30	0.00	0.40	167	1.3	31	-579.71	0.40	-1353.08	1.30	168.15	0.50
GJ 754	19 20 47.95	-45 33 28.3	170.25	0.61	-0.35	0.10	169	1.6	24	670.76	0.18	-2893.49	0.25	170.60	0.62
GJ 1236	19 22 02.07	+07 02 31.0	92.74	1.25	-2.16	0.43	92.9	2.5	1	-731.53	0.41	-438.96	0.63	94.90	1.32
LP 869-19	19 42 00.65	-21 04 05.2	53.14	0.63	-0.54	0.11				76.66	0.25	-243.99	0.67	53.68	0.64
LP 870-65	20 04 30.78	-23 42 01.9	54.86	0.55	-0.03	0.14				120.43	0.32	-330.14	0.38	54.89	0.57
LP 695-72	20 24 15.04	-04 15 32.1	26.46	1.19	0.27	0.29				274.49	0.34	-205.03	2.27	26.19	1.22
GJ 1251	20 28 03.83	-76 40 16.4	77.28	0.48	0.00	0.40	79	2.2	24	723.71	0.12	-1218.30	0.36	77.28	0.62
	20 28 20.35	+00 52 26.6	33.21	1.29	-0.04	0.26				96.50	0.93	-6.05	2.04	33.25	1.32
LHS 3566	20 39 23.79	-29 26 33.6	55.66	0.68	-0.39	0.13	57.3	2.7	3	319.30	0.17	-723.67	0.48	56.05	0.69
GJ 1256	20 40 33.64	+15 29 57.2	104.61	0.96	-0.20	0.24	101.5	1.7	1,29	1308.54	0.32	666.53	0.46	104.81	0.99
GJ 810 B	20 55 37.07	-14 03 54.6	78.70	0.64	-0.35	0.27	82.79	1.24	25	1409.74	0.16	-448.31	0.25	79.05	0.70
GJ 810A	20 55 37.72	-14 02 07.8	79.24	1.53	0.27	0.32	73.1	1.2	1,25	1408.14	0.36	-452.75	0.55	78.97	1.56
	20 57 54.09	-02 52 30.3	64.55	0.75	-0.16	0.16	70.1	3.7	11	-0.32	0.16	-93.11	0.18	64.71	0.77
	21 04 14.91	-10 37 37.0	56.70	0.86	-0.48	0.32	53	1.71	13	591.99	0.27	-285.09	0.23	57.18	0.92
LHS 504	21 05 14.06	-24 46 50.4	15.71	0.50	-0.15	0.37	12.37	4.43	9	-323.89	0.23	-1035.00	0.49	15.86	0.62
LP 759-17	22 02 11.25	-11 09 46.1	27.44	1.18	0.00	0.40				126.49	0.90	-171.78	0.43	27.44	1.25
Eps Indi B	22 04 10.52	-56 46 57.7	275.32	3.02	0.00	0.40	276.06	0.28	27	3955.59	0.77	-2464.29	12.85	275.32	3.05
GJ 1265	22 13 42.78	-17 41 08.2	96.46	0.47	-0.54	0.18	96	3.90	1	845.63	0.21	-296.07	0.31	97.00	0.50
GJ 4274	22 23 06.97	-17 36 25.0	137.29	0.48	-0.29	0.12	137.7	1.7	1,15	304.11	0.19	-703.52	0.28	137.58	0.50
	22 24 43.81	-01 58 52.1	85.70	0.83	-0.44	0.39	85	1.5	14	470.83	0.19	-857.03	0.21	86.14	0.92
GJ 4281	22 28 54.40	-13 25 17.9	91.21	0.60	-0.61	0.30	88.8	3.9	1	-324.84	0.15	-1032.51	0.16	91.82	0.67
LP 876-10	22 48 04.47	-24 22 07.5	128.86	0.23	-0.71	0.21	132.07	1.17	32	326.08	0.13	-176.05	0.40	129.57	0.31
LHS 3872	22 54 46.49	-05 28 26.2	40.31	0.65	0.41	0.66	42.4	4.5	1,23	607.33	0.31	341.96	1.76	39.91	0.92
GL 877	22 55 45.51	-75 27 31.2	116.86	0.76	0.00	0.40	116.1	1.2	1,27	-1011.79	0.74	-1063.32	1.80	116.86	0.86
	23 06 29.28	-05 02 28.6	79.10	1.11	-0.99	0.36	82.6	2.6	9	922.02	0.61	-461.88	0.94	80.09	1.17

Table 2—Continued

Name	RA	Decl.	$\pi_{\rm rel}$ (mas)	$\sigma\pi_{\rm rel}$ (mas)	Zero Pt (mas)	$\sigma_{\rm ZPt}$ (mas)	$\pi_{\rm Lit.}$ (mas)	$\sigma\pi_{\rm Lit}$ (mas)	Ref	μ_{RA} ($cos\delta$,rel) (mas yr^{-1})	$\sigma\mu$ ($cos\delta$,rel) (mas yr^{-1})	μ_{δ} (rel) (mas yr^{-1})	$\sigma\mu$ (rel) (mas yr^{-1})	$\pi_{\rm abs}$ (mas)	$\sigma\pi_{\rm abs}$ (mas)
LHS 3970	23 33 40.57	-21 33 52.6	43.50	0.46	0.00	0.40				689.82	0.33	-319.82	0.51	43.50	0.61
GJ 1286	23 35 10.50	-02 23 21.4	138.20	0.56	-0.53	0.24	138.3	3.5	1	771.71	0.18	-824.23	0.44	138.73	0.61
GJ 4350	23 36 52.27	-36 28 51.8	84.38	0.50	-0.68	0.98	86.2	2	24	1156.96	0.13	65.82	0.25	85.06	1.10
LHS 3992	23 39 18.89	-20 56 55.8	9.12	0.68	0.47	0.52				668.46	0.26	-280.00	0.42	8.65	0.86
LEHPM 6494	23 56 10.81	-34 26 04.4	52.86	0.57	-0.26	0.34	52.37	1.71	13	80.52	0.24	-302.87	0.13	53.12	0.66
LP 880-140	23 59 03.89	-29 32 22.7	44.59	1.66	3.99	2.49				-232.39	0.37	235.13	2.38	40.60	2.99

Note. — Literature parallaxes are weighted averages when more than one value exists
(Table 2 will be published online in its entirety in a machine readable format. The published paper will show a stub table for guidance regarding its form and content.)

References. — [1] van Altena et al. (1995); [2] Tinney et al. (1995); [3] Costa et al. (2005); [4] Harrington & Dahn (1980); [5] Dahn et al. (1988); [6] Dahn et al. (2002); [7] Dahn et al. (1982); [8] Henry et al. (2006); [9] Costa et al. (2006); [10] Riedel et al. (2010); [11] Faherty et al. (2012); [12] Tinney (1996); [13] Dieterich et al. (2014); [14] Vrba et al. (2004); [15] Riedel et al. (2014); [16] Marocco et al. (2013); [17] Gatewood (2008); [18] Riedel et al. (2011); [19] Andrei et al. (2011); [20] Heintz (1994); [21] Ianna & Fredrick (1995); [22] Anglada-Escudé et al. (2012); [23] Smart et al. (2010); [24] Jao et al. (2005); [25] Jao et al. (2011); [26] Deacon & Hambly (2001); [27] van Leeuwen (2007); [28] Harrington et al. (1993); [29] Deacon et al. (2005); [30] Dupuy & Liu (2012); [31] Pravdo & Shaklan (2009); [32] Mamajek et al. (2013);